J. Fluid Mech. (2014), *vol.* 755, R6, doi:10.1017/jfm.2014.423

JFM RAPIDS
journals.cambridge.org/rapids

Spectral eddy viscosity of stratified turbulence

Sebastian Remmler† and Stefan Hickel

Institute of Aerodynamics and Fluid Mechanics, Technische Universität München, 85747 Garching bei München, Germany

(Received 2 April 2014; revised 10 July 2014; accepted 17 July 2014; first published online 18 August 2014)

The spectral eddy viscosity (SEV) concept is a handy tool for the derivation of large-eddy simulation (LES) turbulence models and for the evaluation of their performance in predicting the spectral energy transfer. We compute this quantity by filtering and truncating fully resolved turbulence data from direct numerical simulations (DNS) of neutrally and stably stratified homogeneous turbulence. The results qualitatively confirm the plateau–cusp shape, which is often assumed to be universal, but show a strong dependence on the test filter size. Increasing stable stratification not only breaks the isotropy of the SEV but also modifies its basic shape, which poses a great challenge for implicit and explicit LES methods. We find indications that for stably stratified turbulence it is necessary to use different subgrid-scale (SGS) models for the horizontal and vertical velocity components. Our data disprove models that assume a constant positive effective turbulent Prandtl number.

Key words: homogeneous turbulence, stratified turbulence, turbulence modelling

1. Introduction

In large-eddy simulation (LES) the unresolved part of the turbulent velocity field is modelled by a subgrid-scale (SGS) model. This SGS turbulence model is supposed to modify the flow energy balance in the same way as the small-scale structures of fully resolved turbulence would do. Most SGS models are, at least to some extent, based on an eddy viscosity hypothesis. This means that the SGS model dissipates turbulence energy, especially at the smallest resolved scales, but also on larger scales. Heisenberg (1948) introduced the concept of modelling nonlinear interactions in turbulence by a scale-dependent spectral eddy viscosity (SEV). The underlying theory has since been refined by Kraichnan (1976) and others. Although impractical in real-space-based numerical simulations, the SEV as a function of wavenumber can be used to verify the correct behaviour of SGS models in a set-up of homogeneous (but not necessarily isotropic) turbulence.

† Email address for correspondence: remmler@tum.de

© Cambridge University Press 2014

Downloaded from http://www.cambridge.org/core. Technical University of Munich University Library, on 16 Sep 2016 at 05:07:35, subject to the Cambridge Core terms of use, available at http://www.cambridge.org/core/terms. http://dx.doi.org/10.1017/jfm.2014.423

Algebraic expressions for the SEV have been derived based on the eddy-damped quasi-normal Markovian (EDQNM) theory (Orszag 1970) for isotropic turbulence. A different approach was pursued by Domaradzki *et al.* (1987), who computed the SEV from direct numerical simulations (DNS) of fully resolved turbulence by truncating the results in spectral space. They found some agreement with the theoretical results of Kraichnan (1976), but also differences due to the finite inertial range in their simulations. Despite these discrepancies, the behaviour of isotropic turbulence is quite well understood. On the other hand, corresponding numerical studies for anisotropic turbulence are still rare.

Semi-analytical expressions for the eddy-viscosity and eddy-diffusivity spectra for stratified turbulence are given by Godeferd & Cambon (1994), Staquet & Godeferd (1998) and Godeferd & Staquet (2003) in the framework of the EDQNM approximation. Another form was obtained by Sukoriansky, Galperin & Staroselsky (2005) and Galperin & Sukoriansky (2010) through quasi-normal scale elimination (QNSE). These theoretical results show that turbulence anisotropy can significantly affect SGS energy dissipation in flows dominated by stable stratification, solid body rotation or shear.

In validating an SGS model for stably stratified flows, we have generated an extensive database of DNS results for homogeneous stratified turbulence. The simulations cover a wide range of Froude numbers from the neutrally stratified to the strongly stratified regime (Remmler & Hickel 2012, 2013). We now analyse these results with respect to the anisotropic, i.e. direction-dependent, SEV. To achieve this, we follow Domaradzki *et al.* (1987) and filter the DNS results to coarser resolutions in several steps and compute the SGS stress necessary to obtain the same large-scale result on the coarse grid as on the full DNS grid. Similar studies were presented by Kitsios, Frederiksen & Zidikheri (2012, 2013) for the quasi-geostrophic equations and by Khani & Waite (2013) for the Boussinesq equations using one-dimensional SEV spectra based on grid truncation in the horizontal or vertical direction.

In the following section, we will briefly outline the governing equations, review the concept of SEV and diffusivity and comment on our flow solver. A short overview of the computational set-up follows. The results section presents results for isotropic turbulence in comparison to the work of Kraichnan (1976) and Domaradzki *et al.* (1987) as well as SEV data in a two-dimensional spectral space for stably stratified homogeneous turbulence. Furthermore, we use these newly obtained reference data to evaluate the performance of different existing LES methods. One model follows the implicit LES paradigm, i.e. the discretisation scheme and the SGS model are merged. The other models combine an explicit approximation of the SGS tensor with a non-dissipative central discretisation.

2. Computational methods

2.1. *Boussinesq equations*

The flows to be investigated are characterised by a stable background stratification, so the density is not constant. However, the density differences are small and the flow velocities are much smaller than the speed of sound, which justifies the Boussinesq approximation. The non-dimensional Boussinesq equations for a stably stratified fluid in Cartesian coordinates read

$$\boldsymbol{\nabla}\cdot\boldsymbol{u} = 0, \tag{2.1a}$$

$$\partial_t\boldsymbol{u} + \boldsymbol{\nabla}\cdot(\boldsymbol{u}\boldsymbol{u}) = -\boldsymbol{\nabla}p - \frac{\rho}{Fr_0^2}\hat{\boldsymbol{e}}_z + \frac{1}{Re_0}\nabla^2\boldsymbol{u} + \boldsymbol{F}, \tag{2.1b}$$

Downloaded from http://www.cambridge.org/core. Technical University of Munich University Library, on 16 Sep 2016 at 05:07:35, subject to the Cambridge Core terms of use, available at http://www.cambridge.org/core/terms. http://dx.doi.org/10.1017/jfm.2014.423

$$\partial_t \rho + \boldsymbol{\nabla} \cdot (\rho \boldsymbol{u}) = \boldsymbol{u} \cdot \hat{\boldsymbol{e}}_z + \frac{1}{Pr\, Re_0} \nabla^2 \rho, \tag{2.1c}$$

where the velocities are made non-dimensional by a reference velocity $\mathscr{U}$, all spatial coordinates by the length scale $\mathscr{L}$, pressure by $\overline{\rho}\mathscr{U}^2$, time by $\mathscr{L}/\mathscr{U}$ and density fluctuation $\rho = \rho^* - \overline{\rho}$ (ρ^* is the local absolute density, $\overline{\rho}$ is the background density) by the background density gradient $\mathscr{L}|\mathrm{d}\overline{\rho}/\mathrm{d}z|$. The vertical unit vector is $\hat{\boldsymbol{e}}_z$ and $\boldsymbol{F}$ denotes a large-scale forcing, see (3.1). The non-dimensional flow parameters are

$$Fr_0 = \frac{\mathscr{U}}{N\mathscr{L}}, \quad Re_0 = \frac{\mathscr{U}\mathscr{L}}{\nu}, \quad Pr = \frac{\nu}{D}, \tag{2.2a–c}$$

where ν is the kinematic viscosity, $N = \sqrt{-g/\overline{\rho}\,\mathrm{d}\overline{\rho}/\mathrm{d}z}$ is the Brunt–Väisälä frequency and D is the thermal diffusivity of the fluid. We chose a Prandtl number of $Pr = 0.7$, corresponding to typical values in the atmosphere.

The local dissipation rates ε_k and ε_p of kinetic energy $E_k = (1/2)\sum_i u_i u_i$ and available potential energy $E_p = (1/2)\rho^2/Fr_0^2$ can be computed directly from the velocity and density field,

$$\varepsilon_k = \frac{\boldsymbol{u} \cdot \nabla^2 \boldsymbol{u}}{Re_0}, \quad \varepsilon_p = \frac{\rho \nabla^2 \rho}{Pr\, Re_0\, Fr_0^2}. \tag{2.3a,b}$$

With the spatial mean values of kinetic energy $\langle E_k \rangle$ and kinetic energy dissipation $\langle \varepsilon_k \rangle$, we define the local Froude and Reynolds number as well as the buoyancy Reynolds number $\mathscr{R}$, (Brethouwer *et al.* 2007)

$$Fr = \frac{Fr_0 \mathscr{L}}{\mathscr{U}} \frac{\langle \varepsilon_k \rangle}{\langle E_k \rangle}, \quad Re = \frac{Re_0}{\mathscr{U}\mathscr{L}} \frac{\langle E_k \rangle^2}{\langle \varepsilon_k \rangle}, \quad \mathscr{R} = Re\, Fr^2, \tag{2.4a–c}$$

which are used to characterise the flow regime. The overturning wavenumber (Dougherty 1961; Ozmidov 1965)

$$k_O = \frac{N^{3/2}}{\varepsilon_k^{1/2}} \tag{2.5}$$

approximately separates small scales which are practically isotropic and large scales which are affected by buoyancy.

2.2. *Spectral eddy viscosity*

The momentum equation for incompressible homogeneous turbulence in spectral space reads

$$\left(\partial_t + \nu k^2\right) \hat{u}_i(\boldsymbol{k}) = \hat{S}_i(\boldsymbol{k}) - \mathrm{i} \sum_{j,q} k_q P_{ij}(\boldsymbol{k}) \sum_{\boldsymbol{m}} \hat{u}_j(\boldsymbol{m}) \hat{u}_q(\boldsymbol{k} - \boldsymbol{m}), \tag{2.6}$$

where $P_{ij}(\boldsymbol{k}) = \delta_{ij} - k_i k_j / k^2$ is the projection tensor onto a divergence-free velocity field, δ_{ij} is the Kronecker symbol, $k^2 = |\boldsymbol{k}|^2 = k_1^2 + k_2^2 + k_3^2$ is the wavenumber and $\hat{S}_i$ contains all forces on the fluid. The kinetic energy of a single mode $\boldsymbol{k}$ is

$$e_i(\boldsymbol{k}) = \tfrac{1}{2} \hat{u}_i(\boldsymbol{k}) \hat{u}_i^\star(\boldsymbol{k}), \tag{2.7}$$

where $(\cdot)^\star$ denotes the complex conjugate. Implicit summation over repeated indices does not apply throughout this paper. If required, summation is directly indicated. We refer to $e(\boldsymbol{k}) = \sum_i e_i(\boldsymbol{k})$ as the total kinetic energy and to $e_h(\boldsymbol{k}) = e_1(\boldsymbol{k}) + e_2(\boldsymbol{k})$ and

Downloaded from http:/www.cambridge.org/core. Technical University of Munich University Library, on 16 Sep 2016 at 05:07:35, subject to the Cambridge Core terms of use, available at http:/www.cambridge.org/core/terms. http://dx.doi.org/10.1017/jfm.2014.423

$e_v(\boldsymbol{k}) = e_3(\boldsymbol{k})$ as the horizontal and vertical kinetic energy, respectively (assuming for simplicity that the vertical direction coincides with the x_3 direction).

The temporal evolution of $e_i(\boldsymbol{k})$ is governed by

$$\left(\partial_t + 2\nu k^2\right) e_i(\boldsymbol{k}) - \mathrm{Re}\left\{\hat{S}_i \hat{u}_i^\star(\boldsymbol{k})\right\} = T_i(\boldsymbol{k}), \tag{2.8}$$

with the transfer term

$$T_i(\boldsymbol{k}) = \sum_{j,q} k_q P_{ij}(\boldsymbol{k}) \mathrm{Im}\left\{\sum_{\boldsymbol{m}} \hat{u}_i^\star(\boldsymbol{k}) \hat{u}_j(\boldsymbol{m}) \hat{u}_q(\boldsymbol{k}-\boldsymbol{m})\right\}. \tag{2.9}$$

If the numerical discretisation acts as a perfect low-pass filter, only wavenumbers $|\boldsymbol{k}| < k_c$ are resolved and we can split the transfer term $T(\boldsymbol{k})$ into

$$T(\boldsymbol{k}) = \sum_i T_i(\boldsymbol{k}) = T^-(\boldsymbol{k}, k_c) + T^+(\boldsymbol{k}, k_c); \quad |\boldsymbol{k}| < k_c, \tag{2.10}$$

where $T^-(\boldsymbol{k}, k_c)$ involves only interactions of wavenumbers $|\boldsymbol{k}| < k_c$, $|\boldsymbol{m}| < k_c$, $|\boldsymbol{k}-\boldsymbol{m}| < k_c$ and is thus resolved by the numerical grid. The SGS transfer $T^+(\boldsymbol{k}, k_c)$ represents all unresolved interactions and has to be modelled in an LES.

We can model the average SGS transfer by using the SEV hypothesis

$$\nu_t(k, k_c) = \frac{\left\langle T^+(\boldsymbol{k}, k_c)\right\rangle_s}{2k^2 \left\langle e(\boldsymbol{k})\right\rangle_s} \quad \text{or} \quad \nu_t(\boldsymbol{k}', k_c) = \frac{\left\langle T^+(\boldsymbol{k}, k_c)\right\rangle_c}{2k^2 \left\langle e(\boldsymbol{k})\right\rangle_c}. \tag{2.11a,b}$$

The average $\langle\cdots\rangle_s$ is taken over time and on thin spherical shells with radius $|\boldsymbol{k}|$ for isotropic turbulence, which reduces the wavenumber space to one dimension k. For flows with spectra symmetric about the k_z-axis, such as rotating or stratified turbulence, we average $\langle\cdots\rangle_c$ over thin cylindrical shells with radius $k_h = |\boldsymbol{k}_h| = \sqrt{k_x^2 + k_y^2}$. The result is defined in a two-dimensional wavenumber space $\boldsymbol{k}' = (k_h, k_z)$. We compute the SEV for the horizontal and vertical kinetic energy by

$$\nu_{t,h} = \frac{1}{4k^2}\left[\frac{\left\langle T_1^+\right\rangle}{\langle e_1\rangle} + \frac{\left\langle T_2^+\right\rangle}{\langle e_2\rangle}\right]; \quad \nu_{t,v} = \frac{\left\langle T_3^+\right\rangle}{2k^2 \langle e_3\rangle}. \tag{2.12a,b}$$

For isotropic turbulence the SEV is generally normalised by the cutoff wavenumber and the kinetic energy at this wavenumber

$$\nu_t^+(k/k_c) = \nu_t(k, k_c)\sqrt{\frac{k_c}{E(k_c)}}, \tag{2.13}$$

where the integral kinetic energy is $E(k) = 4\pi k^2 \langle e(\boldsymbol{k})\rangle$. This is only a useful definition if the energy spectrum is known (e.g. $E(k) = C_K \varepsilon^{2/3} k^{-5/3}$) at the cutoff wavenumber. Otherwise, it is helpful to use the original formulation of Kraichnan (1976),

$$\nu_t^*(k/k_c) = \nu_t(k, k_c)\varepsilon_k^{-1/3} k_c^{4/3}. \tag{2.14}$$

For isotropic turbulence with an infinite inertial range, ν_t^+ and ν_t^* are simply related by $\nu_t^* = \sqrt{C_K}\nu_t^+$, where C_K is the Kolmogorov constant. An algebraic model equation for $\nu_t^+(k/k_c)$ in isotropic turbulence is given by Chollet (1984).

As we have a fully resolved simulation of homogeneous turbulence, we can extract the full transfer term $T(\boldsymbol{k})$. By filtering the solution to a coarser test grid, we find the resolved term $T^-(\boldsymbol{k}, k_c)$ for the test grid resolution and then compute the SGS transfer $T^+(\boldsymbol{k}, k_c)$ from (2.10).

Downloaded from http://www.cambridge.org/core. Technical University of Munich University Library, on 16 Sep 2016 at 05:07:35, subject to the Cambridge Core terms of use, available at http://www.cambridge.org/core/terms. http://dx.doi.org/10.1017/jfm.2014.423

We can derive an expression for the spectral eddy diffusivity (SED) of any conserved scalar, such as the density fluctuation

$$D_t(\boldsymbol{k}', k_c) = \frac{\left\langle T_p^+(\boldsymbol{k}, k_c)\right\rangle_c}{2k^2\left\langle e_p(\boldsymbol{k})\right\rangle_c}, \tag{2.15}$$

where T_p^+ is the SGS transfer term in the density equation and

$$e_p(\boldsymbol{k}) = \tfrac{1}{2}\hat{\rho}(\boldsymbol{k})\hat{\rho}^\star(\boldsymbol{k}) \tag{2.16}$$

is the spectral potential energy density. We normalise the SED by

$$D_t^*(k/k_c) = D_t(k, k_c)\varepsilon_k^{-1/3}k_c^{4/3} \tag{2.17}$$

using the kinetic energy dissipation rate ε_k as for the SEV. This normalisation follows from the common belief that the eddy diffusivity can roughly be modelled with a turbulent Prandtl number, which is backed by spectral turbulence theory for high Reynolds numbers and Prandtl numbers of order unity (see equation (23) in Hickel, Adams & Mansour 2007).

We define the effective turbulent Prandtl number for a certain cutoff wavenumber k_c in the spectral space,

$$Pr_t(\boldsymbol{k}, k_c) = \frac{\nu_t(\boldsymbol{k}, k_c)}{D_t(\boldsymbol{k}, k_c)}. \tag{2.18}$$

2.3. *Flow solver*

With our flow solver INCA, the Boussinesq equations are discretised by a fractional-step method on a staggered Cartesian mesh. For time advancement the explicit third-order Runge–Kutta scheme of Shu (1988) is used. The time step is dynamically adapted to satisfy a Courant–Friedrichs–Lewy condition (including the limits for advective, diffusive and buoyancy terms) with CFL $\leqslant 1.0$. The Poisson equation for the pressure is solved at every Runge–Kutta substep.

2.4. *Spatial discretisation and SGS models*

The spatial discretisation is based on a finite-volume method. We use a non-dissipative central-difference scheme with second-order accuracy for the diffusive terms and the pressure Poisson solver. The discretisation of the advective terms depends on the application. For the DNS we use a non-dissipative fourth-order central difference scheme (CDS4).

For LES on much coarser grids a turbulence SGS model is required. In the present study we tested four different SGS models. The first model is the Adaptive Local Deconvolution Method (ALDM). It is an implicit SGS model, i.e. the numerical discretisation of the advective terms acts as a sink of energy by providing a suitable amount of numerical dissipation. This is achieved by a reconstruction of the unfiltered solution through an approximate deconvolution and a regularisation based on a tailored numerical flux function. ALDM was developed by Hickel, Adams & Domaradzki (2006) and Hickel *et al.* (2007) and successfully applied to stably stratified turbulent flows by Remmler & Hickel (2012, 2013).

Alternatively, an explicit SGS model can be applied on top of the non-dissipative central discretisation scheme. We use the Smagorinsky (1963) model with a fixed

Downloaded from http:/www.cambridge.org/core. Technical University of Munich University Library, on 16 Sep 2016 at 05:07:35, subject to the Cambridge Core terms of use, available at http:/www.cambridge.org/core/terms. http://dx.doi.org/10.1017/jfm.2014.423

No.	Re	Fr	$\mathscr{R}$	Re_λ	ηk_{max}	k_O
1	20 800	∞	∞	372	0.95	0.0
2	23 150	0.089	184.0	393	0.97	6.4
3	28 250	0.025	17.2	434	0.83	38.4
4	33 480	0.008	2.1	472	0.71	192.0

TABLE 1. List of the presented DNS ordered by the strength of the stable stratification. No. 1 is neutrally stratified, No. 4 is strongly stratified.

model coefficient of $C_S = 0.18$ ('standard Smagorinsky model', SSM) or a dynamic version of this model ('dynamic Smagorinsky model', DSM) based on the dynamic procedure proposed by Germano *et al.* (1991) and improved by Lilly (1992). The dynamic procedure is used to compute the Smagorinsky model coefficient based on test filtering the numerical solution assuming scale similarity between the smallest resolved scales and the largest unresolved scales. The test filter size is twice the grid size. For numerical stability reasons the computed model coefficient is usually averaged in homogeneous directions. Since we investigate a flow field that is homogeneous in all three directions, the method reduces to the computation of a spatially constant but temporally varying model coefficient. We also investigated the case without spatial averaging; this is denoted 'DSM2' in § 4. In order to prevent numerical instability, the Smagorinsky model coefficient is clipped if negative values are computed. The turbulent Prandtl number is assumed to be $Pr_t = 0.4$ for both the SSM and the DSM.

3. Numerical set-up

We simulated homogeneous stratified turbulence in a triply periodic box with side length $\mathscr{L} = 2\pi$ and a resolution of 512^3 cells. A fluctuating large-scale horizontal volume force is applied to the fluid, which injects a constant forcing power into the domain. The time- and space-dependent forcing term reads (Aspden *et al.* 2008)

$$\boldsymbol{F}(\boldsymbol{x}, t) = \sum_{i,j=1}^{2} \boldsymbol{a}_{i,j} \cos(2\pi k_i x + p_{i,j}) \cos(2\pi k_j y + q_{i,j}). \tag{3.1}$$

The random amplitudes $\boldsymbol{a}_{i,j}$ and phases $p_{i,j}$ and $q_{i,j}$ are recomputed at every time step. After an initial transient phase, the turbulence kinetic energy remains at a constant level, as soon as the forcing power $P = 1/(2\pi)$ is balanced by the mean molecular dissipation $\varepsilon_k + \varepsilon_p$. A more detailed description of the simulations is provided by Remmler & Hickel (2013). We sampled the SEV and SED in time intervals $\Delta T = 5\mathscr{L}/\mathscr{U}$ sufficiently large to ensure decorrelated velocity and density fields. With an average computational time step of $\Delta t = 1.6 \times 10^{-3}\mathscr{L}/\mathscr{U}$ we needed ~3125 time steps for each sample. To limit computational costs, we restricted ourselves to 20 samples per simulation. All figures presented below are averages of these samples.

A list of the simulations can be found in table 1, where we provide the non-dimensional parameters for each case as well as the Reynolds number based on the Taylor microscale (see, e.g. Pope 2000), computed using the kinetic energy E_k and kinetic energy dissipation ε_k,

$$Re_\lambda = E_k \sqrt{\frac{20 Re_0}{3\mathscr{U}\mathscr{L}\varepsilon_k}}. \tag{3.2}$$

Downloaded from http://www.cambridge.org/core. Technical University of Munich University Library, on 16 Sep 2016 at 05:07:35, subject to the Cambridge Core terms of use, available at http://www.cambridge.org/core/terms. http://dx.doi.org/10.1017/jfm.2014.423

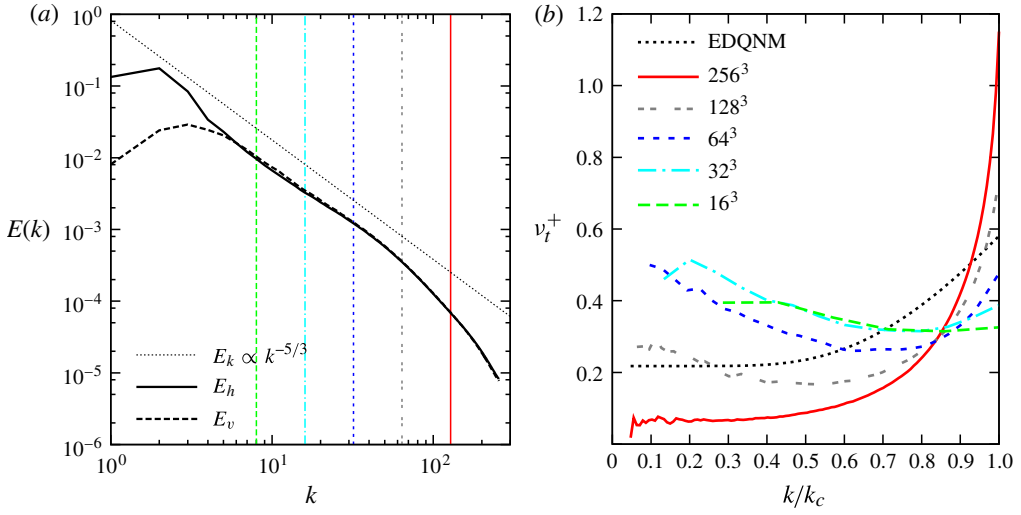

FIGURE 1. Integrated spectra of neutrally stratified turbulence DNS (512^3 cells). (*a*) Horizontal and vertical kinetic energy spectra. The vertical lines indicate cutoff wavenumbers for SEV computation. (*b*) SEV at different test grid levels. The EDQNM prediction (Kraichnan 1976) is also shown for comparison.

The product of the Kolmogorov length η and the maximum resolved wavenumber k_{max} is $\eta k_{max} \approx 1$, which indicates sufficient resolution of the smallest scales of turbulence.

The Ozmidov wavenumber k_O indicates the smallest scales of motion that are affected by buoyancy. For case No. 2 only the largest scales are affected by buoyancy; in case No. 4 almost the complete spectrum is influenced by buoyancy forces. (It should be noted that the grid cutoff wavenumber is $k_c = 256$.)

4. Results and discussion

4.1. *Neutrally stratified turbulence*

For neutrally stratified turbulence we can compare our results directly with the EDQNM prediction. The spectra of horizontal and vertical kinetic energy shown in figure 1(*a*) confirm that the turbulence is fully isotropic for wavenumbers $k > 5$. In figure 1(*b*) we show the results of spherically averaged SEV for five different coarse test grids together with the algebraic law of Kraichnan. It turns out that in our simulations the values of ν_t^+ are similar to the theoretical ones and the plateau–cusp shape of the curve is reproduced. However, the cusp is sharper than in the theoretical curve and its maximum value increases with the test grid resolution. Moreover, the plateau at low wavenumbers is tilted, its level rises with decreasing test grid resolution and it saturates for the test grid with 64^3 cells and the coarser grids.

Domaradzki *et al.* (1987) already observed a lower level of the SEV at low wavenumbers compared with theory, when they analysed DNS of isotropic turbulence at very low Reynolds number. Therefore the low-level plateau is probably due to the high cutoff wavenumbers which are close to the dissipative range.

The dependence of the cusp maximum and sharpness on the test grid was also observed and quantified by Kitsios *et al.* (2012). Our observations confirm their findings.

Downloaded from http:/www.cambridge.org/core. Technical University of Munich University Library, on 16 Sep 2016 at 05:07:35, subject to the Cambridge Core terms of use, available at http:/www.cambridge.org/core/terms. http://dx.doi.org/10.1017/jfm.2014.423

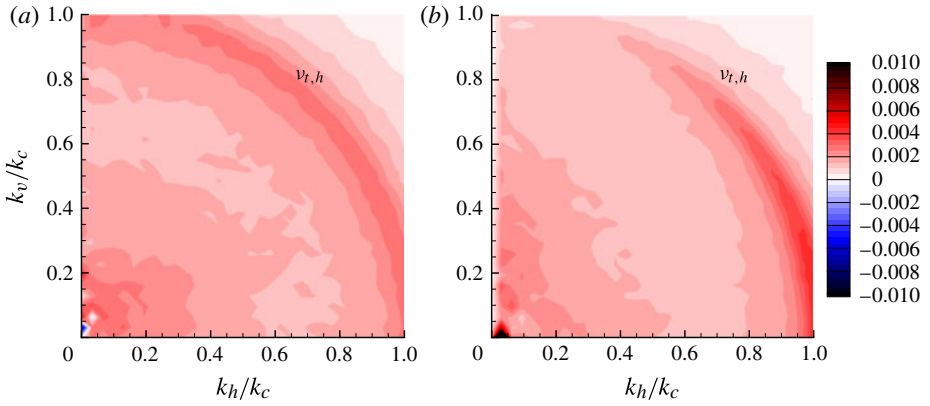

FIGURE 2. Two-dimensional SEV of neutrally stratified horizontally forced turbulence (test grid with 64^3 cells). Horizontal (a) and vertical (b) kinetic energy.

In figure 2 we present the SEV in a two-dimensional spectral space. Averaging was performed on circles with constant distance from the vertical axis. The analysis was carried out separately for the horizontal and vertical kinetic energy components. It turns out that, as expected, the horizontal eddy viscosity spectrum $\nu_{t,h}$ shows an isotropic distribution. The SEV of the vertical kinetic energy component $\nu_{t,v}$ is not isotropic, which is due to the anisotropic spectrum of any single-direction kinetic energy in a divergence-free velocity field.

4.2. *Stably stratified turbulence*

We applied the same analysis to the simulations with stable stratification, see figure 3. In this case, a third type of energy has to be considered, the available potential energy and hence the SED D_t. In the following, it is sometimes helpful to discuss the results not in Cartesian spectral coordinates but in terms of the absolute wavenumber k and the angle ϕ, which has the range $0 \leqslant \phi \leqslant \pi/2$ for the horizontal and vertical directions, respectively.

The cutoff wavenumber for the spectra presented in figure 3 is $k_c = 32$. This means that it is larger than the Ozmidov wavenumber k_O in case No. 2, approximately equal to k_O in case No. 3 and significantly smaller than k_O in case No. 4. As pointed out by Khani & Waite (2013), this has a large influence on the SEV and SED spectra.

The SEV of the horizontal kinetic energy is still almost isotropic in case No. 2 with $\mathscr{R} = 184$. At lower Froude numbers the cusp no longer appears in all directions, but only at medium angles ϕ. At the lowest Froude number investigated, it almost completely vanishes.

For the vertical kinetic energy, there is no visible difference between the neutral and the weakly stratified case. With increasing stable stratification, the overall level of $\nu_{t,v}$ decreases and a region with negative values appears. This could be explained by an inverse energy cascade or by the effect of 'pancake' vortices elongated in the horizontal direction and layered in the vertical direction. Remmler & Hickel (2013) indeed observed a transport of vertical kinetic energy from small to larger vertical scales in the case of strong stable stratification (cf. their figure 4b), which supports this view.

The SED differs quite strongly from the SEV described above. In the weakly stratified case, there is a clear plateau–cusp behaviour, but the plateau level depends

Downloaded from http://www.cambridge.org/core. Technical University of Munich University Library, on 16 Sep 2016 at 05:07:35, subject to the Cambridge Core terms of use, available at http://www.cambridge.org/core/terms. http://dx.doi.org/10.1017/jfm.2014.423

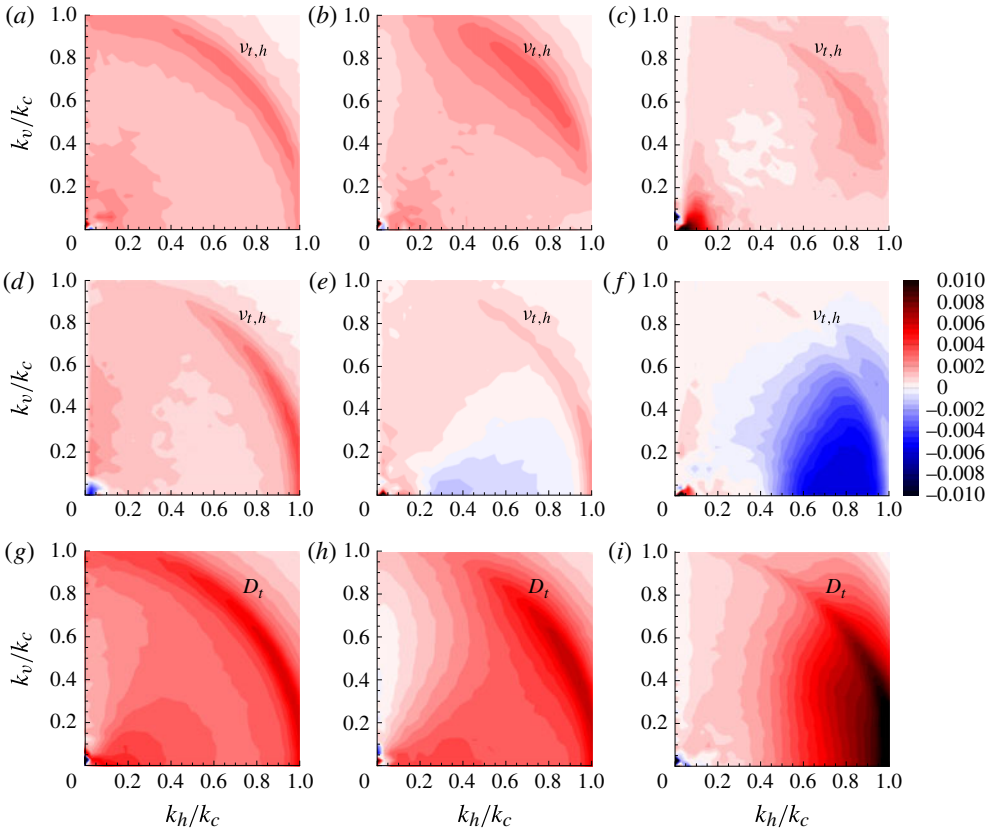

FIGURE 3. SEV and diffusivity of stably stratified turbulence (test grid with 64^3 cells) at different Froude numbers (corresponding to weak, medium and strong stratification). Horizontal (*a–c*) and vertical (*d–f*) kinetic energy as well as potential energy (*g–i*). (*a*,*d*,*g*) $\mathscr{R} = 184$, $Fr = 0.089$; (*b*,*e*,*h*) $\mathscr{R} = 17.2$, $Fr = 0.025$; (*c*,*f*,*i*) $\mathscr{R} = 2.1$, $Fr = 0.008$.

on the spectral direction. It strongly decreases when ϕ is increased. The cusp level, in contrast, is almost unaffected by the spectral direction. It decreases only slightly at $\phi \approx \pi/2$. Case No. 3 ($\mathscr{R} = 17.2$) looks very similar, just the plateau level is decreased and the drop of the cusp level at high ϕ is more pronounced than in the previous case. For the strongest stratification, the picture changes significantly. There is a peak at high horizontal wavenumbers and no plateau region as in the previous cases.

According to Galperin & Sukoriansky (2010), the horizontal viscosity and diffusivity should grow in the case of increased stratification while the vertical counterparts decrease. Our results confirm this for the vertical viscosity and diffusivity, but show a different trend for the horizontal direction.

The effective turbulent Prandtl number (figure 4) is homogeneously distributed in the spectrum in the case of weak stratification. In the horizontal direction there is a plateau at $Pr_t \approx 0.35$ and a cusp near the cutoff wavenumber with a maximum value of $Pr_t = 0.55$. For the vertical direction $Pr_t > 1$. In the case of stronger stratification the difference in the horizontal and vertical directions is increased, leading to a large region with negative values in our most strongly stratified case. The growth of the vertical turbulent Prandtl number with increasing stratification, at least for cases Nos 2 and 3, is in agreement with the findings of Galperin & Sukoriansky (2010).

Downloaded from http:/www.cambridge.org/core. Technical University of Munich University Library, on 16 Sep 2016 at 05:07:35, subject to the Cambridge Core terms of use, available at http:/www.cambridge.org/core/terms. http://dx.doi.org/10.1017/jfm.2014.423

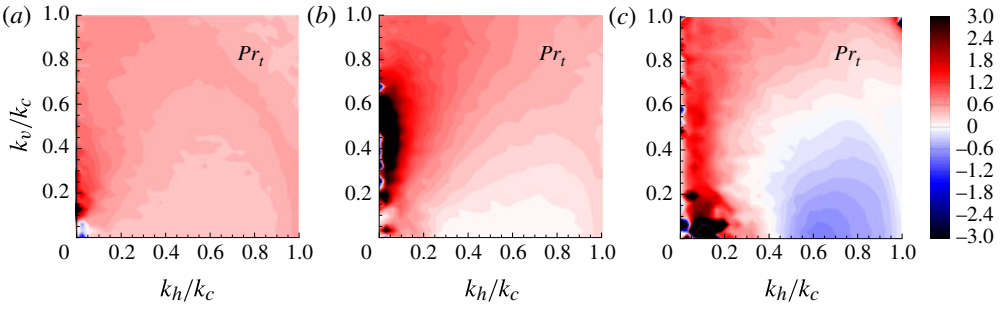

FIGURE 4. Effective turbulent Prandtl number in stably stratified turbulence (test grid with 64^3 cells) at different Froude numbers (corresponding to weak, medium and strong stratification). (*a*) $\mathscr{R} = 184$, $Fr = 0.089$; (*b*) $\mathscr{R} = 17.2$, $Fr = 0.025$; (*c*) $\mathscr{R} = 2.1$, $Fr = 0.008$.

Based on the observed inhomogeneity of the effective turbulent Prandtl number in spectral space we conclude that traditional SGS models assuming a constant positive turbulent Prandtl number are certainly unsuitable for simulations of strongly stratified turbulence.

4.3. *Analysis of LES schemes*

The reference data obtained from filtering the DNS can now be used to analyse LES methods. We computed the effective SEV and SED in LES from an ensemble of statistically independent snapshots of the flow field (see Hickel *et al.* 2006). The SEV and SED are both affected by the numerical discretisation and the turbulence SGS model. Both interfere with each other and cannot be judged independently, which motivates the idea of implicit LES where the discretisation and the SGS model are fully merged. Since quantitative comparison of two-dimensional plots as in figures 2 and 3 is difficult, we show the SEV and SED of different LES methods in figure 5 in a one-dimensional graph that is a cut through the spectral space at $\phi = \pi/4$ (the 'diagonal' modes). As a test case we selected case No. 3 with a medium stable stratification. The cutoff wavenumber $k_c = 16$ is slightly smaller than the Ozmidov wavenumber $k_O = 38.4$, so the SGS turbulence is, to a certain degree, influenced by buoyancy forces. Together with the EDQNM prediction and the DNS reference result, we show the results obtained with the ALDM, pure CDS4 without an SGS model and CDS4 with explicit models, namely SSM, DSM and DSM2.

It turns out that none of the tested methods are able to correctly reproduce all three SEV and SED spectra at the same time. The ALDM does on average a good job, which is remarkable since the method was optimised to reproduce the EDQNM curve as closely as possible (Hickel *et al.* 2006). The averaged DSM gives good results for the SEV of the horizontal kinetic energy and the SED of the available potential energy, but fails for the SEV of the vertical kinetic energy. The SEV of the vertical kinetic energy, on the other hand, is well predicted by the pure CDS4 discretisation without a turbulence SGS model. The DSM2 model, which allows for local variations in the model coefficient, does not improve the result over the averaged DSM, but rather makes it worse.

5. Summary and conclusions

We have computed the SEV and diffusivity of homogeneous turbulence with and without stable stratification. This was achieved by filtering fully resolved DNS results

Downloaded from http://www.cambridge.org/core. Technical University of Munich University Library, on 16 Sep 2016 at 05:07:35, subject to the Cambridge Core terms of use, available at http://www.cambridge.org/core/terms. http://dx.doi.org/10.1017/jfm.2014.423

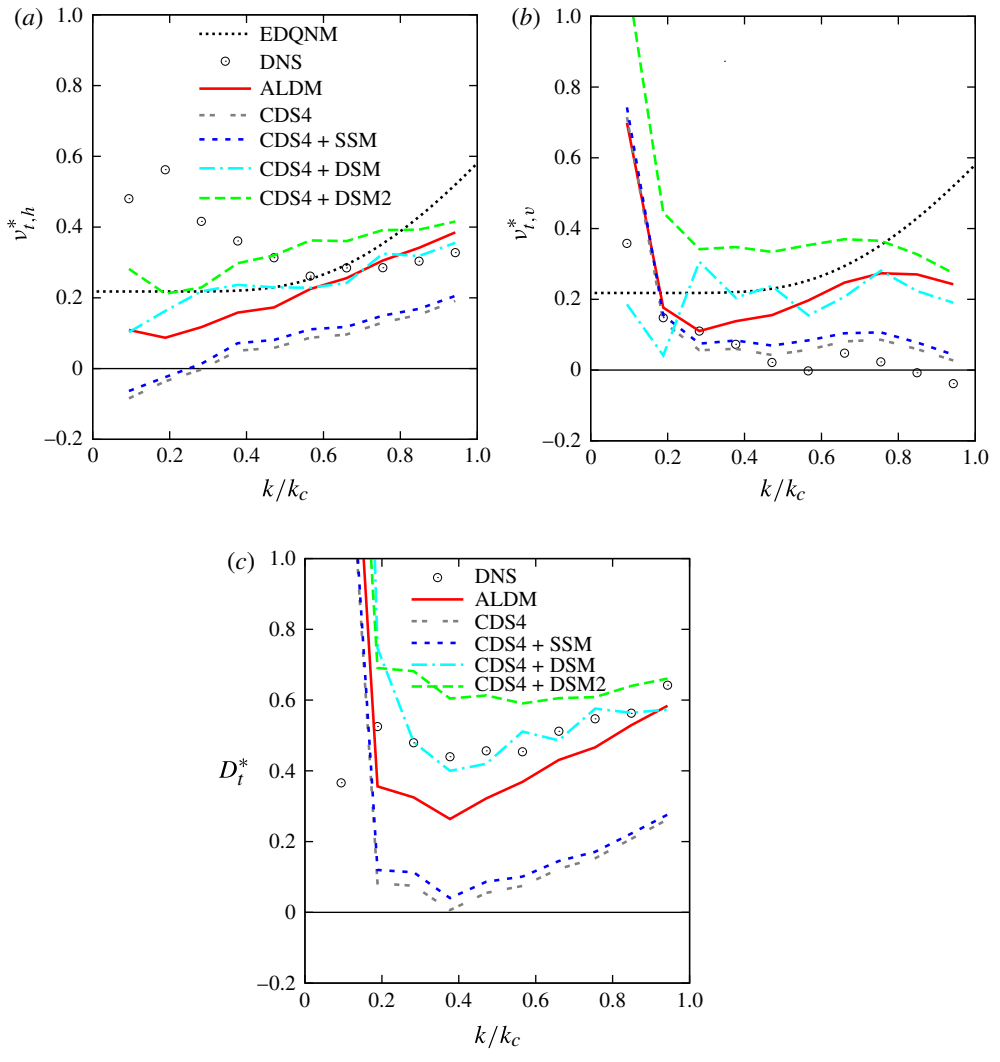

FIGURE 5. Diagonal SEV and SED of stably stratified turbulence at $\mathscr{R} = 17.2$ (32^3 cells) computed with different discretisation schemes and turbulence SGS models. (*a*) $\nu^*_{t,h}$; (*b*) $\nu^*_{t,v}$; (*c*) D^*_t.

and by computing the additional spectral energy flux that is necessary to obtain the same total flux in the coarse-grained flow field as in the fully resolved case.

For neutrally stratified turbulence we found eddy viscosity spectra that are, in general, similar to the EDQNM prediction of Kraichnan (1976) showing the well-known plateau–cusp behaviour. However, the amplitude of the cusp at the cutoff wavenumber depends on the test filter size, as described by Kitsios *et al.* (2012), and at low wavenumbers we find a pronounced linear decrease of the SEV instead of a flat plateau.

If the stable stratification is increased, the SEV and SED spectra become more and more anisotropic. For the most stable case investigated, the spectral space topology has completely changed. This illustrates that the characteristics of the flow change significantly as soon as the buoyancy Reynolds number approaches $\mathscr{R} \approx 1$. Strong

Downloaded from http:/www.cambridge.org/core. Technical University of Munich University Library, on 16 Sep 2016 at 05:07:35, subject to the Cambridge Core terms of use, available at http:/www.cambridge.org/core/terms. http://dx.doi.org/10.1017/jfm.2014.423

stratification leads to negative values of the effective turbulent Prandtl number at large horizontal and small vertical wavenumbers. Such results contradict the widespread assumption of a constant positive effective turbulent Prandtl number in SGS modelling. The treatment of SGS stresses in such cases must generally be different from that in fully turbulent flows with higher values of $\mathscr{R}$.

We used the results from the filtered DNS to test the implicit SGS model ALDM and a central discretisation scheme with and without the Smagorinsky model, either in the standard form or in the dynamic form. We found that the ALDM, despite being calibrated for the SEV from EDQNM theory, yields acceptable results for all three forms of flow energy. The DSM does a good job except for the vertical kinetic energy, which is best matched by the central discretisation without any SGS model. These results suggest that a potentially better model could be obtained by applying the DSM only to the horizontal velocity components and leaving the vertical momentum equation unmodified.

Acknowledgements

This work was funded by the German Research Foundation (DFG) under the grant HI 1273-1 in the framework of the MetStröm priority programme (SPP 1276). Computational resources were provided by the High Performance Computing Center Stuttgart (HLRS) under the grant TIGRA.

References

ASPDEN, A. J., NIKIFORAKIS, N., DALZIEL, S. B. & BELL, J. B. 2008 Analysis of implicit LES methods. *Commun. Appl. Math. Comput. Sci.* **3** (1), 103–126.

BRETHOUWER, G., BILLANT, P., LINDBORG, E. & CHOMAZ, J.-M. 2007 Scaling analysis and simulation of strongly stratified turbulent flows. *J. Fluid Mech.* **585**, 343–368.

CHOLLET, J.-P. 1984 Two-point closures as a subgrid scale modeling for large eddy simulations. In *4th Symposium on Turbulent Shear Flows* (ed. H. Viets, R. J. Bethke & D. Bougine), p. 9.

DOMARADZKI, J. A., METCALFE, R. W., ROGALLO, R. S. & RILEY, J. J. 1987 Analysis of subgrid-scale eddy viscosity with use of results from direct numerical simulations. *Phys. Rev. Lett.* **58** (6), 547–550.

DOUGHERTY, J. P. 1961 The anisotropy of turbulence at the meteor level. *J. Atmos. Sol.-Terr. Phys.* **21**, 210–213.

GALPERIN, B. & SUKORIANSKY, S. 2010 Geophysical flows with anisotropic turbulence and dispersive waves: flows with stable stratification. *Ocean Dyn.* **60**, 1319–1337.

GERMANO, M., PIOMELLI, U., MOIN, P. & CABOT, W. H. 1991 A dynamic subgrid-scale eddy viscosity model. *Phys. Fluids* A **3** (7), 1760–1765.

GODEFERD, F. S. & CAMBON, C. 1994 Detailed investigation of energy transfers in homogeneous stratified turbulence. *Phys. Fluids* **6** (6), 2084–2100.

GODEFERD, F. S. & STAQUET, C. 2003 Statistical modelling and direct numerical simulations of decaying stably stratified turbulence. Part 2. Large-scale and small-scale anisotropy. *J. Fluid Mech.* **486**, 115–159.

HEISENBERG, W. 1948 Zur statistischen Theorie der Turbulenz. *Z. Phys.* A **124**, 628–657.

HICKEL, S., ADAMS, N. A. & DOMARADZKI, J. A. 2006 An adaptive local deconvolution method for implicit LES. *J. Comput. Phys.* **213**, 413–436.

HICKEL, S., ADAMS, N. A. & MANSOUR, N. N. 2007 Implicit subgrid-scale modeling for large-eddy simulation of passive scalar mixing. *Phys. Fluids* **19**, 095102.

KHANI, S. & WAITE, M. L. 2013 Effective eddy viscosity in stratified turbulence. *J. Turbul.* **14** (7), 49–70.

KITSIOS, V., FREDERIKSEN, J. S. & ZIDIKHERI, M. J. 2012 Subgrid model with scaling laws for atmospheric simulations. *J. Atmos. Sci.* **69** (4), 1427–1445.

Downloaded from http://www.cambridge.org/core. Technical University of Munich University Library, on 16 Sep 2016 at 05:07:35, subject to the Cambridge Core terms of use, available at http://www.cambridge.org/core/terms. http://dx.doi.org/10.1017/jfm.2014.423

KITSIOS, V., FREDERIKSEN, J. S. & ZIDIKHERI, M. J. 2013 Scaling laws for parameterisations of subgrid eddy–eddy interactions in simulations of oceanic circulations. *Ocean Model.* **68**, 88–105.

KRAICHNAN, R. H. 1976 Eddy viscosity in two and three dimensions. *J. Atmos. Sci.* **33**, 1521–1536.

LILLY, D. K. 1992 A proposed modification of the German subgrid-scale closure method. *Phys. Fluids* A **4** (3), 633–635.

ORSZAG, S. A. 1970 Analytical theories of turbulence. *J. Fluid Mech.* **41** (02), 363–386.

OZMIDOV, R. V. 1965 On the turbulent exchange in a stably stratified ocean. *Izv., Atmos. Ocean. Phys.* **1**, 493–497.

POPE, S. B. 2000 *Turbulent Flows*. Cambridge University Press.

REMMLER, S. & HICKEL, S. 2012 Direct and large eddy simulation of stratified turbulence. *Intl J. Heat Fluid Flow* **35**, 13–24.

REMMLER, S. & HICKEL, S. 2013 Spectral structure of stratified turbulence: direct numerical simulations and predictions by large eddy simulation. *Theor. Comput. Fluid Dyn.* **27**, 319–336.

SHU, C.-W. 1988 Total-variation-diminishing time discretizations. *SIAM J. Sci. Stat. Comput.* **9** (6), 1073–1084.

SMAGORINSKY, J. 1963 General circulation experiments with the primitive equations. I: The basic experiment. *Mon. Weath. Rev.* **91**, 99–164.

STAQUET, C. & GODEFERD, F. S. 1998 Statistical modelling and direct numerical simulations of decaying stably stratified turbulence. Part 1. Flow energetics. *J. Fluid Mech.* **360**, 295–340.

SUKORIANSKY, S., GALPERIN, B. & STAROSELSKY, I. 2005 A quasinormal scale elimination model of turbulent flows with stable stratification. *Phys. Fluids* **17** (8), 085107.

Downloaded from http:/www.cambridge.org/core. Technical University of Munich University Library, on 16 Sep 2016 at 05:07:35, subject to the Cambridge Core terms of use, available at http:/www.cambridge.org/core/terms. http://dx.doi.org/10.1017/jfm.2014.423